

Ionization Potentials of Tantalum–Carbide Clusters: An Experimental and Density Functional Theory Study

Viktoras Dryza, M. A. Addicoat, Jason R. Gascooke, Mark A. Buntine, and Gregory F. Metha*

Department of Chemistry, The University of Adelaide, South Australia 5005, Australia

Received: August 8, 2005; In Final Form: September 28, 2005

We have used photoionization efficiency spectroscopy to determine the ionization potentials (IP) of the tantalum–carbide clusters, Ta_3C_n ($n = 1–3$) and Ta_4C_n ($n = 1–4$). The ionization potentials follow an overall reduction as the number of carbon atoms increases; however, the trend is not steady as expected from a simple electrostatic argument. Instead, an oscillatory behavior is observed such that clusters with an odd number of carbon atoms have higher IPs and clusters with an even number of carbon atoms have lower IPs, with the Ta_4C_4 cluster exhibiting the lowest IP. Excellent agreement is found with relative IPs calculated using density functional theory for the lowest energy structures, which are consistent with the development of a $2 \times 2 \times 2$ face-centered nanocrystal. This work shows that IPs may be used as a reliable validation for the geometries of metal–carbide clusters calculated by theory. The variation in IP can also be interpreted qualitatively with application of a simple model based upon isolobal frontier orbitals.

I. Introduction

The coupling of laser ablation, supersonic expansions, and mass spectrometry has nurtured the growth of studies into clusters containing refractive metals and other elements such as carbon, nitrogen, and oxygen. Consequently, much has been learned about the structures and bonding arrangements for various gas-phase metal–ligand clusters.^{1–4} The Group 5 metal–carbide clusters have been shown to adopt either one of two bonding motifs: metallocarbohedrenes or “met-cars”, (M_8C_{12}) made up of 8 metal atoms and 12 carbon atoms, and cubic crystalline structures or “nanocrystals” (e.g., $M_{14}C_{13}$) made up of approximately equal numbers of metal and carbon atoms. Work by the Castleman and Duncan groups has shown that vanadium–carbon and niobium–carbon clusters (neutral and ionic) form both met-car and nanocrystal structures under a variety of conditions.^{2,3,5–8} In contrast, Castleman and co-workers have shown that the next Group 5 element, tantalum, forms metal–carbide clusters exclusively with stoichiometries that are consistent with face-centered cubic nanocrystals (e.g., $Ta_{14}C_{13}$, and $Ta_{24}C_{24}$).⁹ Experimental work by us on neutral tantalum–carbon clusters suggests the formation and enhanced stability of the smallest possible type of tantalum–carbon nanocrystal, Ta_4C_4 .¹⁰ Our supporting DFT calculations show that the structure of Ta_4C_4 consists of a distorted tetrahedron of Ta atoms with a C atom bonded to each of the four faces.

Recent collaborative work by Meijer, von Helden, and Duncan and co-workers has shown that infrared spectral information can be obtained for transition-metal carbide clusters via the application of IR-MPI using a tuneable infrared free electron laser.^{11–14} The clusters are excited to energies at which they undergo delayed ionization, a process enhanced on vibrational resonances that relate to molecular structure. For example, vastly different spectra are observed for the Ti_8C_{12} met-car compared to the $Ti_{14}C_{13}$ nanocrystal.^{11,12} The former

has a strong absorbance near 1400 cm^{-1} that is attributed to C–C bonding and the latter absorbs at 500 cm^{-1} and 650 cm^{-1} , which is attributed to Ti–C bonding. Further work on vanadium–, niobium–, and tantalum–carbide clusters show resonances around 500 and 650 cm^{-1} .^{13,14} The observed frequencies are similar to the IR-active phonon modes of the metallic NbC (100) and TaC (100) surfaces and is direct evidence for the proposed nanocrystalline structure of $M_{14}C_{13}$ clusters. Although Nb_4C_4 and Ta_4C_4 only show a single resonance at 650 cm^{-1} , the spectra are still consistent with these species existing as a $2 \times 2 \times 2$ cubic structure.

Apart from these IR-MPI data, no other spectroscopic information exists for clusters containing both tantalum and carbon atoms. Further spectroscopic investigations of various sized Ta_nC_m clusters are required to gain an understanding of how the structural, electronic, optical, and chemical properties evolve with cluster composition and size. To help address this deficiency, we have employed single-photon photoionization efficiency (PIE) experiments to determine the ionization potentials (IP) of these clusters. As well as being intrinsically important quantities, where shifts in IPs (relative to the pure clusters) can provide information about cluster–absorbate interactions, knowledge of variations in IP is also essential for experiments involving ionization (such as ZEKE or MATI). In concert with the PIE experiments, we have used density functional theory (DFT) to calculate globally minimized structures of the cationic tantalum–carbide clusters. Together with the neutral structures we have calculated previously,¹⁰ we predict the adiabatic ionization energies for comparison with the experimental data.

II. Experimental and Computational Methods

A. Experiment. The experimental details of the laser ionization experiments are similar, but not identical to, those reported previously.¹⁰ Briefly, the tantalum–carbide clusters are formed in a supersonic laser ablation source coupled to a time-

* Corresponding author. E-mail: greg.metha@adelaide.edu.au. Phone: +61 8 8303 5943. Fax: +61 8 8303 4358.

of-flight mass spectrometer (TOFMS). A gas mix consisting of 0.01% acetylene seeded in helium is reacted with the ablation products of a tantalum rod and is passed along a 15-mm-long “condensation tube” before being expanded into the first vacuum chamber. The clusters pass through a home-built skimmer into the second chamber that contains a standard Wiley–McLaren TOFMS arranged perpendicularly with the cluster beam source. The neutral clusters are ionized with the frequency-doubled output of a Nd:YAG-pumped dye laser. Because of inefficiencies in the dye laser grating near 425 nm (Wood’s anomaly), data points between 210 and 214 nm are recorded using the 1st anti-Stokes output from a Raman-shifter operating with H₂. All data points are collected at 0.2-nm intervals, and a typical scan is of 1–2 hour duration. The resultant ions are detected by a double multichannel plate detector, amplified $\times 125$ (Stanford SR445) and sent to a digital oscilloscope (LeCroy 9350 AM, 500 MHz) for averaging (1000 laser shots) before being sent to a PC for analysis. The time taken to average each mass spectrum (100 s at 10 Hz) corresponds to one complete translation/rotation of the tantalum rod. Typical laser powers used are around 50 $\mu\text{J}/\text{pulse}$, collimated to a 5-mm-diameter beam, as measured using an Ophir Nova II power meter. Under these conditions, all ion signals are found to be linearly dependent with laser fluence. During each wavelength (PIE) scan, the laser power is maintained at the predetermined value by controlling the angle of the frequency doubling crystal. Only data collected within $\pm 7\%$ of 50 $\mu\text{J}/\text{pulse}$ were accepted, otherwise the crystal angle was retuned and further data collected at that wavelength. For each data point, normalization was then performed to further reduce the effect of laser power. To check that long-term drift in the cluster concentration does not occur, the laser is returned to the starting wavelength immediately after each scan to ensure that the cluster signal intensity had remained constant. Overlapping scans across different laser dye regions were concatenated by scaling the cluster signal intensities until they were consistent.

B. Computation. Geometry optimization and harmonic vibrational frequency calculations were performed using DFT in the Gaussian 98 suite of programs.¹⁵ The calculations were performed with the B3P86 method using the LANL2DZ basis set. The LANL2DZ basis set employs the Dunning/Huzinaga double- ξ descriptor for the carbon atoms and replaces the core electrons of tantalum (up to 4f) with the effective core potentials of Hay and Wadt.^{16,17} This method and basis set are the same as those used by us previously, albeit with an earlier version of the program (i.e., Gaussian 94), to calculate structures of various neutral tantalum–carbide, Ta_mC_n ($m = 1-4$, $n = 0-4$), clusters.¹⁰ In that case, only clusters having singlet (even number of Ta atoms) and doublet (odd number of Ta atoms) multiplicities were explored. In a recent paper on mixed-metal clusters including Ta₄,¹⁸ and this work, we have included an examination of higher multiplicities (triplets, quartets, quintets, and sextets). All structures were initially optimized without any geometry constraint. All minima were characterized with vibrational frequency calculations to determine whether the optimized structure was a true minimum. The globally minimized structure for each stoichiometry was then examined to determine any symmetry properties, and the calculations were repeated again within the highest symmetry point group. The symmetry-constrained energy was subsequently compared to the unconstrained energy to ensure that there was no difference. Following this, harmonic vibrational frequencies were also recalculated within the point group to determine the frequency and symmetry of each normal mode of vibration. Occasionally, the higher-symmetry calculation could not be made to converge. In these

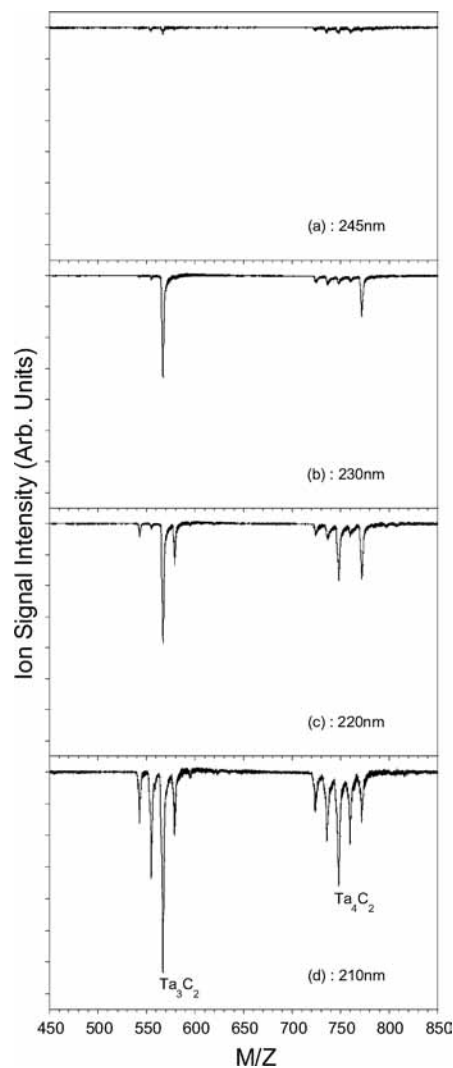


Figure 1. Mass spectra of Ta₃C_n and Ta₄C_n clusters at four different ionization wavelengths.

cases we still assume the higher symmetry point group but it is denoted with an asterisk (e.g., C_{2v}*). For each optimized structure, the Mulliken charge population and bonding population (density terms involving pairs of basis functions on different centers) were calculated. Bonding and antibonding interactions are indicated by positive and negative values, respectively. For all structures presented in this report, bonds are drawn between atoms when the Mulliken bonding population is calculated to be ≥ 0.070 (this corresponds approximately to Ta–Ta bond lengths ≤ 2.8 Å and Ta–C bond lengths ≤ 2.1 Å).

III. Results and Discussion

A. Ionization Potential Measurements. Figures 1a–d show a portion of the mass spectra of tantalum–carbide clusters following ionization at four different wavelengths; 245, 230, 220, and 210 nm, respectively, under otherwise identical conditions. In the spectrum recorded at 210 nm (Figure 1d) Ta₃ clusters appear with 0–3 carbon atoms and Ta₄ clusters with 0–4 carbon atoms attached; peaks corresponding to Ta₃C₂ and Ta₄C₂ are labeled. All of these species are produced following single-photon ionization. In contrast, the spectrum recorded at 245 nm (Figure 1a) shows that the intensity of all species has decreased dramatically to near baseline levels. At this wavelength, none of the species are ionized with one photon and the residual signal is due to multiple photon absorption leading to

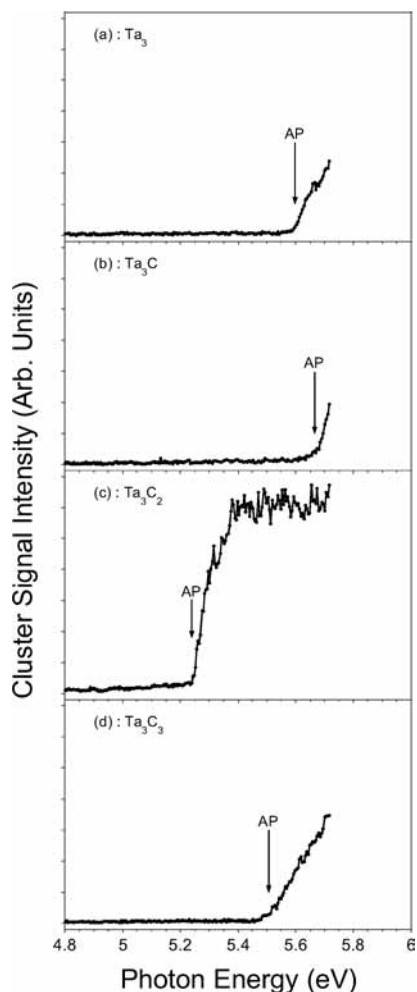


Figure 2. Photoionization efficiency spectra for Ta_3C_n clusters. The arrows indicate the onset of ionization (appearance potential) for each cluster.

ionization, and possibly fragmentation. Although these peaks could be diminished completely by lowering the laser power, we found this was not possible without severely affecting the S/N of the other spectra. Following ionization at 230 nm (Figure 1b), the Ta_3C_2 and Ta_4C_4 clusters display dramatically increased intensity. At 220 nm (Figure 1c), the Ta_3 , Ta_3C_3 , and Ta_4C_2 clusters appear. Finally back to 210 nm, the clusters Ta_3C , Ta_4C , and Ta_4C_3 are now present. From this data, it is obvious that there are significant differences between the wavelengths at which specific clusters become ionized.

Photoionization efficiency (PIE) spectra were recorded by monitoring the signal of each cluster as a function of wavelength. The PIE spectra for the Ta_3C_n ($n = 0-3$) and Ta_4C_n ($n = 0-4$) clusters are shown in Figure 2a-d and Figure 3a-e, respectively. It is immediately apparent that the Ta_3C_2 and Ta_4C_4 clusters exhibit the lowest IPs for the Ta_3C_n and Ta_4C_n series, respectively. Furthermore, most clusters show a dramatic rise from the baseline (e.g., Ta_3C , Ta_3C_2 , and Ta_4C_2), indicating good Franck-Condon overlap between the electronic states of the neutral and cation. In contrast, the Ta_4C_4 cluster exhibits a gradual onset of ionization, suggesting significant geometry change between the neutral and cation. Appearance potentials (AP) were determined by the intersection of two fitted lines on each PIE trace; one to the linear portion of the rising slope and the other to the baseline. This approach simplifies the data, is internally consistent, and has an estimated error of ± 0.05 eV. Because of the internal energy of the molecular beam, IPs

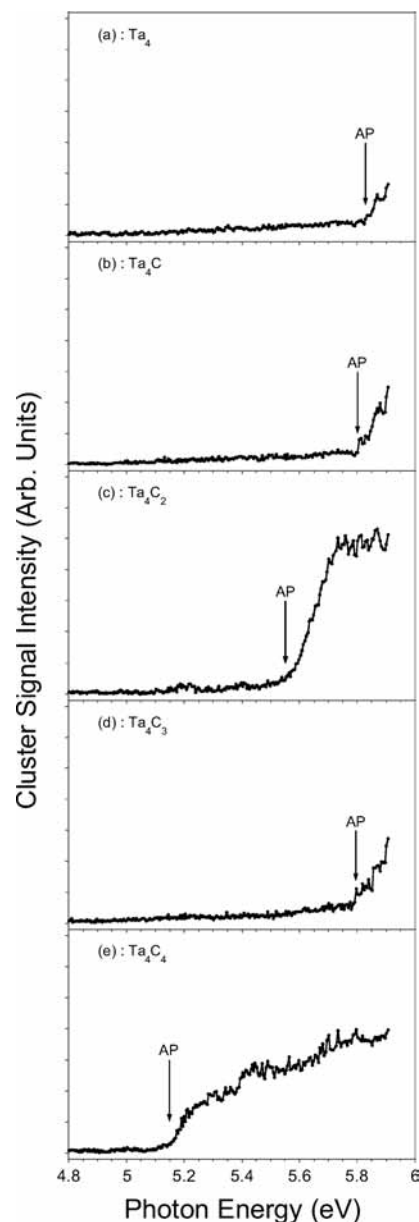


Figure 3. Photoionization efficiency spectra for Ta_4C_n clusters. The arrows indicate the onset of ionization (appearance potential) for each cluster.

determined from PIE spectroscopy have absolute errors of ~ 0.1 eV. The appearance potentials were then converted to ionization potentials after converting to vacuum wavenumber and correcting for the residual static field in the extraction electrodes using the term $\text{IP} - \text{AP} = 6.1 \times E^{1/2}$ (in cm^{-1} with E in V/cm) as recommended by Schlag and co-workers.¹⁹ As a check, the ionization energies extracted for Ta_3 and Ta_4 are found to be in good agreement with those determined previously.²⁰

The resultant IPs determined for each of the Ta_3C_n (\blacktriangle) and Ta_4C_n (\blacksquare) clusters are plotted in Figure 4 as a function of the numbers of carbon atoms attached to each cluster and are also listed in the second column of Table 1. First, it can be seen that Ta_4 has an IP that is 0.23 eV higher than Ta_3 (5.83 cf. 5.60 eV), which has been found previously.²⁰ This behavior is not unusual for transition-metal clusters in the small-size regime where the IPs do not drop monotonically with cluster size but rather are highly irregular. The IP of the vanadium tetramer is 0.16 eV higher than the trimer (5.66 cf. 5.50 eV), although the reverse is true in the case of niobium clusters (5.64 cf. 5.81

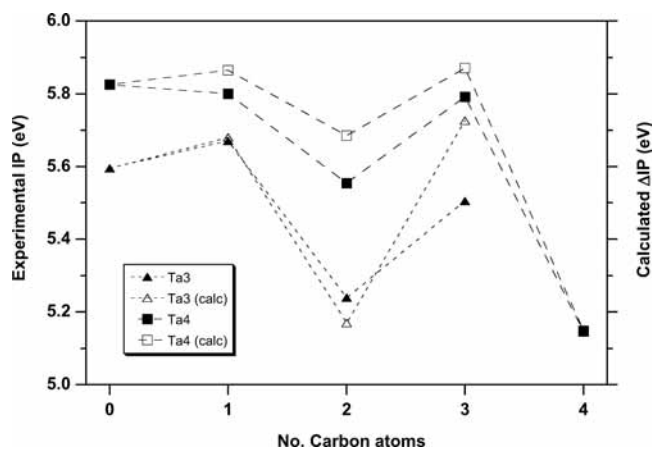


Figure 4. Experimental values of IP for Ta_3C_n and Ta_4C_n clusters as a function of n . Also shown on the same scale are relative values, ΔIP , calculated using DFT.

TABLE 1: Experimental Ionization Potentials Observed for Ta_3C_n , Ta_4C_n ^a

cluster	exptl IP	calculated transition	calculated IP (exc. ZPE)	calculated IP (inc. ZPE)
Ta_3	5.60	$S = 3/2 \rightarrow S = 1$	6.228	6.267
Ta_3C	5.67	$S = 1/2 \rightarrow S = 0$	6.341	6.352
"		$S = 1/2 \rightarrow S = 1$	6.921	6.923
"		$S = 3/2 \rightarrow S = 1$	6.977	7.002
Ta_3C_2	5.24	$S = 1/2 \rightarrow S = 0$	5.823	5.841
Ta_3C_3	5.51	$S = 1/2 \rightarrow S = 0$	6.371	6.398
Ta_4	5.83	$S = 0 \rightarrow S = 1/2$	6.230	6.218
Ta_4C	5.80	$S = 0 \rightarrow S = 1/2$	6.260	6.258
Ta_4C_2	5.55	$S = 0 \rightarrow S = 1/2$	6.080	6.078
Ta_4C_3	5.79	$S = 0 \rightarrow S = 1/2$	6.264	6.264
Ta_4C_4	5.15	$S = 1 \rightarrow S = 1/2$	5.527	5.541

^a Also listed are calculated transitions and corresponding ionization potentials for Ta_3C_n and Ta_4C_n clusters.

eV).^{21–24} We also note that Ta_7 and Ta_8 clusters have higher IPs than Ta_6 .²⁰

Upon addition of one and three carbon atoms, very little change in IP is observed for the Ta_3C_n and Ta_4C_n clusters; indeed, the IP of Ta_3C has increased slightly by 0.07 eV. However, addition of two carbon atoms results in an IP reduction of 0.36 and 0.28 eV for the Ta_3C_2 and Ta_4C_2 clusters, respectively. For Ta_3C_3 and Ta_4C_3 , reductions of only 0.09 and 0.04 eV are observed. Addition of four carbon atoms produces the relatively large reduction of 0.68 eV for Ta_4C_4 . Overall, there appears an oscillatory pattern to the IPs where clusters with an odd number of carbon atoms have relatively higher IPs than clusters with an even number.

To our knowledge, there have been no studies on the effect of carbon addition on the IPs of Group 5 metal clusters apart from the PIE and PFI-ZEKE study of Nb_3C_2 by Yang et al.,²⁵ which shows an IP reduction of 0.76 eV, twice the shift we observe for Ta_3C_2 . Unfortunately, no other Nb_3C_n species were explored and so the effect of more or less carbon atoms cannot be compared. In their paper, Yang et al. also report the IPs of Nb_4C_4 and Nb_5C_2 to be 4.43 and 4.59 eV, respectively.²⁵ Again, the IP reduction of 1.17 eV for Nb_4C_4 (relative to Nb_4) is much larger than the reduction of 0.68 eV found for Ta_4C_4 . The IP reduction of 0.85 eV for Nb_5C_2 (relative to Nb_5) is even greater than what we observe for either Ta_3C_2 or Ta_4C_2 .

Although the IP information on carbon addition onto Group 5 clusters is sparse, addition of other ligands is more abundant. Addition of Ar_n to niobium clusters shows a steady lowering of the IP with increasing n .²⁶ This has been accounted for by a

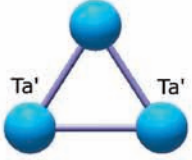
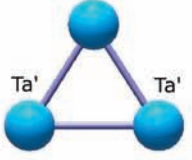
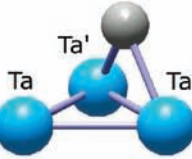
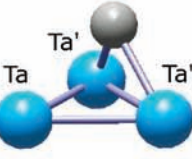
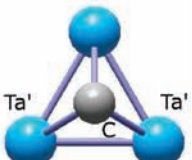
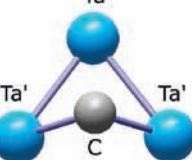
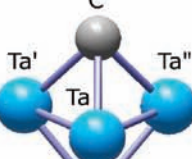
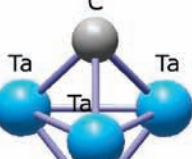
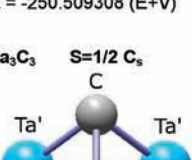
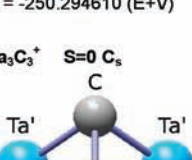
simple electrostatic argument in which the cation experiences a stabilizing charge-induced dipole interaction that lowers the IP.²⁷ In contrast, the effect of adding two hydrogen atoms onto V_m and Nb_m (following dissociative chemisorption of H_2) leads to an increase in IP because of an effective loss of two electrons from the cluster's valence orbitals to form two low-energy metal–hydride bonds.²¹ This effect is observed for the addition of up to four H_2 molecules onto V_4 and Nb_4 . The effect on IP following the addition of oxygen onto niobium clusters has also been examined.²⁴ Addition of one and two oxygen atoms onto Nb_4 results in an IP reduction of 0.3 and 0.03 eV, respectively, which is oscillatory in the opposite sense to the carbon addition observed here. The smallest cluster for which four oxygen atoms is added is Nb_9 , and this shows IP changes of -0.16 , $+0.63$, $+0.10$, and $+0.08$ eV, upon addition of one to four oxygen atoms, respectively.

The data presented in Figure 4 are clearly different from that reported for the sequential addition of other ligands onto Group 5 clusters, and it is tempting to rationalize the IP oscillation in terms of significant geometry change rather than electronic effects. Because the data is oscillatory between even and odd numbers of carbon atoms, it is possible that molecular C_2 units are formed for clusters with two or four carbon atoms. However, we have shown previously with our DFT calculations that the lowest energy structures for tantalum–carbide clusters all have separated carbon atoms.¹⁰ Unfortunately, there are very few experimental structure determinations of metal–carbide clusters, although the structure of the Nb_3C_2 cluster has been elucidated using PFI-ZEKE spectroscopy.²⁵ The cluster has a trigonal bipyramid geometry with two separated carbon atoms bonded to either side of the niobium triangle. Furthermore, the IR-MPI spectrum recorded for Ta_4C_4 does not reveal any vibrational features, suggesting the presence of a molecular C_2 unit.¹⁴ On the basis of this evidence, we postulate that the oscillatory IP pattern does not result from significant geometry changes as more carbon atoms are added. To test this, we look to DFT to calculate the expected IP changes as carbon atoms are added to Ta_3 and Ta_4 . The next section examines the lowest energy structures for neutral and ionic Ta_3C_n ($n = 0–3$) and Ta_4C_n ($n = 0–4$) clusters. Thereafter, we compare the theoretically calculated ionization potentials to those observed experimentally.

B. Calculated Geometries, Electronic States, and Mulliken Populations. We have used DFT previously¹⁰ to calculate the lowest energy structures of neutral Ta_3C_n ($n = 0–3$) and Ta_4C_n ($n = 0–4$), and as part of this work we have reexamined each of the neutral clusters. Using the same procedure as reported previously,¹⁰ we have now calculated the lowest energy structures for the cationic species and consequently determined the adiabatic ionization energy for each cluster. Table 2 shows the calculated lowest energy structure, including symmetry and vibrational frequencies, for Ta_3C_n ($n = 0–3$) neutrals and cations. For neutral and cationic Ta_3C , higher energy structures are also given for the reasons discussed below. Table 3 gives the same information for neutral and cationic Ta_4C_n ($n = 0–4$) clusters. We also present the Mulliken bonding population (number of shared electrons between two atoms) and atomic net charges calculated for each Ta_3C_n and Ta_4C_n cluster. The values for the neutrals and cations are presented together as half matrices in Table 4 (Ta_3C_n) and Table 5 (Ta_4C_n); the neutrals as unbold numbers (bottom LHS) and the cations as bold numbers (upper RHS).

The lowest energy Ta_3 cluster we now find to be a quartet state with an isosceles triangle (C_{2v}^*) structure, which is almost 300 kJ/mol lower in energy than the doublet (C_s) structure we

TABLE 2: Structures, Selected Geometric Parameters, Energies, and Vibrational Frequencies of Neutral (LHS) and Cationic (RHS) Ta_3C_n Clusters

Cluster	Geom. Parameters ^a	Vib. Freq. (cm ⁻¹)	Cluster	Geom. Parameters ^a	Vib. Freq. (cm ⁻¹)
Ta₃ S=3/2 C_{2v}  Ta-Ta' = 2.403 Ta'-Ta' = 2.589 Ta'-Ta-Ta' = 65.2 Ta-Ta'-Ta' = 57.4 E = -174.055243 (E) E = -174.053967 (E+V)	Ta₃⁺ S=1 C_{2v}  Ta-Ta' = 2.425 Ta'-Ta' = 2.505 Ta'-Ta-Ta' = 62.2 Ta-Ta'-Ta' = 58.9 E = -173.825049 (E) E = -173.823631 (E+V)	Ta₃C (I) S=1/2 C_s  Ta-Ta' = 2.441 Ta'-Ta' = 2.613 Ta'-C = 1.966 Ta'-Ta'-Ta = 57.7 Ta'-Ta-Ta' = 64.7 Ta'-C-Ta' = 83.3 Ta'-Ta'-C = 48.3 Ta-Ta'-Ta'-C = 86.8 E = -212.277611 (E) E = -212.272784 (E+V)	Ta₃C⁺ S=0 C_s  Ta-Ta' = 2.450 Ta'-Ta' = 2.671 Ta'-C = 1.950 Ta'-Ta'-Ta = 57.0 Ta'-Ta-Ta' = 66.1 Ta'-C-Ta' = 86.4 Ta'-Ta'-C = 46.8 Ta-Ta'-Ta'-C = 79.8 E = -212.044528 (E) E = -212.039297 (E+V)	Ta₃C (II) S=3/2 C_s  Ta-Ta' = 2.484 Ta'-Ta' = 2.484 Ta-C = 2.082 Ta'-C = 2.091 Ta-Ta'-Ta' = 60.0 Ta'-Ta-Ta' = 60.0 Ta-C-Ta' = 73.1 Ta'-C-Ta' = 72.9 Ta-Ta'-Ta'-C = 64.5 E = -212.279678 (E) E = -212.275677 (E+V)	Ta₃C⁺ S=1 C_s  Ta-Ta' = 2.474 Ta'-Ta' = 2.949 Ta-C = 2.276 Ta'-C = 1.943 Ta-Ta'-Ta' = 53.4 Ta'-Ta-Ta' = 73.2 Ta-C-Ta' = 71.3 Ta'-C-Ta' = 98.7 Ta-Ta'-Ta'-C = 80.8 E = -212.023215 (E) E = -212.018316 (E+V)
Ta₃C₂ S=1/2 C_s  Ta'-Ta'' = 2.612 Ta-Ta' = 2.520 Ta-Ta'' = 2.490 Ta-C = 2.058 Ta'-C = 2.067 Ta''-C = 2.065 Ta-Ta'-Ta'' = 58.0 Ta-Ta''-Ta' = 59.1 Ta'-Ta-Ta'' = 62.8 Ta-Ta''-C = 50.8 Ta-Ta'-C = 52.2 Ta-C-Ta'' = 78.4 Ta-C-Ta' = 75.3 E = -250.517491 (E) E = -250.509308 (E+V)	Ta₃C₂⁺ S=0 D_{3h}  Ta-Ta = 2.520 Ta-C = 2.059 Ta-Ta-Ta = 60.0 Ta-C-Ta = 75.5 Ta-Ta-C = 52.2 E = -250.303460 (E) E = -250.294610 (E+V)	Ta₃C₃ S=1/2 C_s  Ta-Ta' = 2.799 Ta'-Ta' = 2.705 Ta-C = 2.039 Ta'-C = 2.039 Ta'-C' = 1.887 Ta-C' = 1.963 Ta'-C-Ta' = 83.1 Ta'-Ta'-Ta = 61.1 Ta'-Ta-Ta' = 57.8 Ta-C-Ta' = 86.7 Ta'-C'-Ta = 93.2 E = -288.731130 (E) E = -288.717674 (E+V)	Ta₃C₃⁺ S=0 C_s  Ta-Ta' = 2.804 Ta'-Ta' = 2.797 Ta-C = 2.065 Ta'-C = 1.996 Ta'-C' = 1.875 Ta-C' = 1.950 Ta'-C-Ta' = 88.9 Ta'-Ta'-Ta = 60.1 Ta'-Ta-Ta' = 59.8 Ta-C-Ta' = 87.3 Ta'-C'-Ta = 94.3 E = -288.496949 (E) E = -288.482500 (E+V)		


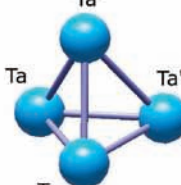
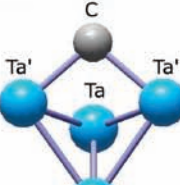
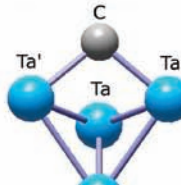
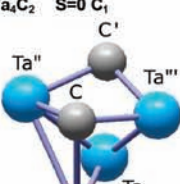
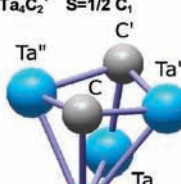
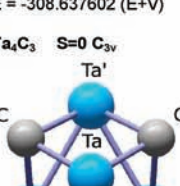
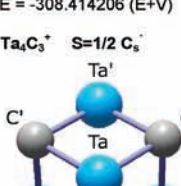
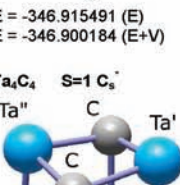
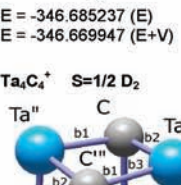
^a Bond lengths in Angstroms, angles in degrees.

reported previously. A Raman study on Ta₃ clusters deposited onto an argon matrix by Lombardi and co-workers reveal a (symmetric) vibration of frequency of 251 cm⁻¹ and postulated a nonequilateral structure that is consistent with both the doublet and quartet state structures.²⁸ The lowest energy Ta₃⁺ cluster is calculated to be a similarly shaped isosceles (C_{2v}^{*}) structure with triplet multiplicity. In the neutral, the Mulliken bonding density is approximately equal between all three bonds.

However, the Ta' and Ta atoms have quite different charges of -0.03 and +0.06, respectively, which results in a shortened Ta-Ta' bond due to electrostatic attraction. Upon ionization, the Ta-Ta' bonding increases, the Ta'-Ta' bonding decreases, the atomic charges on the two Ta' atoms increase by 0.37, and the Ta atom charge increases by 0.25.

For Ta₃C, we have identified a quartet state (C_s) that is only ~5 kJ/mol (450 cm⁻¹) lower in energy than the doublet state

TABLE 3: Structures, Selected Geometric Parameters, Energies, and Vibrational Frequencies of Neutral (LHS) and Cationic (RHS) Ta₄C_n Clusters

Cluster	Geom. Parameters ^a	Vib. Freq. (cm ⁻¹)	Cluster	Geom. Parameters ^a	Vib. Freq. (cm ⁻¹)	
Ta₄ S=0 T _d	Ta-Ta = 2.548 Ta-Ta-Ta = 60.0 φ = 70.5	a ₁ = 286.5 e = 142.6 t ₂ = 203.5		Ta₄⁺ S=1/2 C _{2v}	Ta-Ta' = 2.532 Ta'-Ta' = 2.657 Ta-Ta = 2.564 Ta-Ta'-Ta = 60.8 Ta'-Ta-Ta = 59.6 Ta-Ta'-Ta' = 58.4 Ta'-Ta-Ta' = 63.3 Ta-Ta'-Ta'-Ta = 75.0 Ta'-Ta-Ta'-Ta = 68.8	a ₁ = 130.6, 196.0, 286.2 a ₂ = 138.2 b ₁ = 205.7 b ₂ = 186.0
E = -232.210485 (E) E = -232.207792 (E+V)				E = -231.981484 (E) E = -231.979235 (E+V)		
Ta₄C S=0 C _s	Ta-Ta' = 2.531 Ta'-Ta' = 2.926 Ta-Ta'' = 2.582 Ta'-Ta'' = 2.540 Ta-C = 2.451 Ta'-C = 1.961 Ta-Ta'-Ta' = 54.7 Ta'-Ta-Ta' = 70.6 Ta-C-Ta' = 69.0 Ta-Ta'-Ta'-Ta'' = 77.1 Ta-Ta'-Ta'-C = 90.4 Ta''-Ta'-Ta'-C = 167.5	a' = 129.5, 179.6, 208.1, 267.2, 279.0, 735.1 a'' = 145.4, 186.0, 699.5		Ta₄C⁺ S=1/2 C _s	Ta-Ta' = 2.535 Ta'-Ta' = 2.955 Ta-Ta'' = 2.581 Ta'-Ta'' = 2.589 Ta-C = 2.479 Ta'-C = 1.940 Ta-Ta'-Ta' = 54.4 Ta'-Ta-Ta' = 71.3 Ta-C-Ta' = 68.8 Ta-Ta'-Ta'-Ta'' = 76.1 Ta-Ta'-Ta'-C = 93.6 Ta''-Ta'-Ta'-C = 169.7	a' = 125.6, 165.4, 200.5, 261.3, 280.8, 735.1 a'' = 134.8, 186.2, 717.2
E = -270.431205 (E) E = -270.424759 (E+V)				E = -270.201122 (E) E = -270.194727 (E+V)		
Ta₄C₂ S=0 C ₁	Ta-Ta' = 2.588 Ta-Ta'' = 2.533 Ta-Ta''' = 2.582 Ta'-Ta'' = 2.587 Ta-C' = 2.368 Ta'-C' = 1.959 Ta''-C' = 2.310 Ta''-C' = 1.974 Ta'''-C' = 1.983 Ta'''-C' = 1.963 Ta''-Ta'-Ta-Ta''' = 76.4	a = 103.3, 127.8, 151.6, 163.8, 203.6, 247.9, 263.8, 371.3, 630.7, 704.4, 728.7, 749.9		Ta₄C₂⁺ S=1/2 C ₁	Ta-Ta' = 2.558 Ta-Ta'' = 2.657 Ta-Ta''' = 2.868 Ta'-Ta'' = 2.585 Ta'-Ta''' = 2.641 Ta-C' = 2.025 Ta'-C' = 2.253 Ta''-C' = 1.963 Ta''-C' = 2.119 Ta'''-C' = 1.953 Ta'''-C' = 1.991 Ta''-Ta'-Ta-Ta''' = 72.8	a = 75.7, 117.9, 134.5, 157.5, 206.6, 259.5, 325.4, 434.7, 539.9, 691.2, 706.0, 769.1
E = -308.647728 (E) E = -308.637602 (E+V)				E = -308.424271 (E) E = -308.414206 (E+V)		
Ta₄C₃ S=0 C _{3v}	Ta'-Ta' = 2.579 Ta'-C = 2.076 Ta-C = 1.979 Ta'-Ta'-Ta' = 60.0 Ta'-C-Ta' = 76.8 Ta'-C-Ta = 91.3 Ta'-Ta'-C = 51.6 C-Ta'-C = 85.6 C-Ta-C = 90.9 Ta'-Ta'-Ta'-Ta = 73.4 Ta'-Ta'-Ta'-C = 122.9 Ta-C-C-Ta' = 170.4	e = 142.1, 209.8, 524.0, 590.3, 721.4 a ₁ = 216.1, 263.3, 729.8, 801.3 a ₂ = 337.6		Ta₄C₃⁺ S=1/2 C _s	Ta'-Ta'' = 2.643 Ta''-Ta'' = 2.641 Ta-C = 1.976 Ta-C' = 1.976 Ta'-C' = 2.052 Ta''-C' = 2.053 Ta''-C' = 2.052 Ta-C-Ta'' = 92.0 Ta-C'-Ta' = 92.1 Ta-C'-Ta'' = 92.0 Ta'-Ta''-Ta''-Ta = 72.8 Ta'-C'-C'-Ta = 173.5	a' = 184.3, 214.4, 262.5, 743.8, 818.6 a'' = 125.8, 126.8, 182.6, 354.5, 535.4, 537.0, 582.6, 583.6, 729.6, 730.1
E = -346.915491 (E) E = -346.900184 (E+V)				E = -346.685237 (E) E = -346.669947 (E+V)		
Ta₄C₄ S=1 C _s [*]	Ta-C = 2.005 Ta-C' = 2.057 Ta-C'' = 2.063 Ta'-C' = 2.057 Ta'-C' = 1.991 Ta''-C' = 2.027 Ta''-C'' = 1.972 Ta-C-Ta' = 94.1 Ta-C-Ta'' = 93.7 Ta'-Ta-Ta'' = 64.1 C-C'-C''-C = 80.0	a' = 104.8, 137.2, 212.0, 253.8, 494.0, 547.2, 606.9, 663.7, 688.3, 759.7, 780.8 a'' = 167.2, 206.5, 424.3, 487.9, 584.5, 673.0, 740.5		Ta₄C₄⁺ S=1/2 D ₂	b ₁ = 2.024 b ₂ = 2.031 b ₃ = 1.994 Ta-C''-Ta'' = 93.1 Ta-C''-Ta''' = 88.8 Ta'-Ta'''-Ta-Ta'' = 67.4 C'''-C'-C''-C = 75.6	a = 128.5, 138.5, 266.3, 387.1, 594.6, 770.2 b ₁ = 220.7, 528.1, 676.6, 762.5 b ₂ = 220.0, 535.4, 670.4, 767.7 b ₃ = 194.5, 564.6, 625.6, 712.3
E = -385.119748 (E) E = -385.100310 (E+V)				E = -384.916597 (E) E = -384.896627 (E+V)		

^a Bond lengths in Angstroms, angles in degrees.

reported previously (C_s^{*}). Because of the similarity in energy, details of both the neutral doublet and quartet states are presented in Table 2. Furthermore, we also present the lowest energy singlet and triplet states of the cation (because ionization transitions follow the ΔS = ±1/2 selection rule) in Table 2. The quintet energy is much higher in energy and is not considered.

In Table 4, we have arbitrarily grouped the S = 1/2 neutral and S = 0 cation as system I, and the S = 3/2 neutral and S = 1 cation as system II. (In Table 1, we have included all experimentally possible transitions, that is, from the doublet neutral state, transitions to both the singlet and triplet states of the cation are considered, whereas from the quartet state only

TABLE 4: Summary of Mulliken Bonding Population and Mulliken Charges for Ta₃C_n Neutral (Normal) and Cationic (Bold) Clusters^a

Ta ₃	Ta'	Ta'	Ta		charge (neutral)	charge (cation)
Ta'		0.299	0.398		-0.032	0.341
Ta'	0.339		0.386		-0.032	0.341
Ta	0.325	0.325			0.064	0.317

Ta ₃ C (I)	Ta'	Ta'	Ta	C	charge (neutral)	charge (cation)
Ta'		0.161	0.328	0.272	0.196	0.526
Ta'	0.164		0.328	0.272	0.196	0.526
Ta	0.267	0.267		0.051	0.058	0.420
C	0.320	0.320	0.027		-0.450	-0.472

Ta ₃ C (II)	Ta'	Ta'	Ta	C	charge (neutral)	charge (cation)
Ta'		-0.015	0.388	0.300	0.159	0.542
Ta'	0.210		0.388	0.298	0.159	0.542
Ta	0.212	0.212		0.014	0.162	0.414
C	0.216	0.217	0.223		-0.480	-0.499

Ta ₃ C ₂	Ta'/Ta	Ta''/Ta	Ta	C	C	C	charge (neutral)	charge (cation)
Ta'/Ta		0.114	0.115	0.226	0.226		0.276	0.607
Ta''/Ta	-0.054		0.116	0.226	0.227		0.291	0.607
Ta	0.071	0.124		0.227	0.226		0.370	0.606
C	0.226	0.236	0.261			-0.063	-0.468	-0.410
C	0.226	0.236	0.260	-0.078			-0.469	-0.410

Ta ₃ C ₃	Ta'	Ta'	Ta	C'	C'	C	charge (neutral)	charge (cation)
Ta'		0.122	-0.067	-0.081	0.363	0.175	0.478	0.810
Ta'	0.154		-0.067	0.363	-0.081	0.175	0.478	0.810
Ta	-0.020	-0.020		0.333	0.333	0.173	0.509	0.804
C'	-0.070	0.439	0.356		-0.015	-0.069	-0.476	-0.439
C'	0.439	-0.070	0.356	-0.025		-0.069	-0.476	-0.439
C	0.200	0.200	0.264	-0.076	-0.076		-0.514	-0.546

^a 1st/2nd atom label corresponds to neutral and cation, respectively.

the triplet state is shown.) Despite the similar energies of the two neutral states, the bonding of the carbon atom is significantly different between them. The doublet state has the carbon atom bound to the two Ta' atoms, resulting in a very open dihedral angle of 87°. In contrast, the quartet state has the carbon atom (almost equally) bound to all three Ta atoms giving rise to a closed structure with a dihedral angle of 65°. These differences are reflected clearly in the Mulliken population. In the cation, the singlet state is ~55 kJ/mol lower than the triplet state. Both structures exhibit C_s symmetry and have a doubly bridged C; however, the significant difference is that the Ta'-Ta' bond is antibonding in the triplet state. With respect to the net charge, in system I the Ta' atoms gain 0.33 and the Ta atom gains 0.36 but the carbon atom loses charge, dropping from -0.45 to -0.47 upon ionization. In system II, the Ta' atoms gain 0.38, the Ta atom gains 0.25, and the carbon atom gains 0.02 charge upon ionization.

For Ta₃C₂, the doublet state (C_s^{*}) shown in Table 2 is the same structure as that reported previously.¹⁰ For the cation, the lowest energy state is a singlet state with D_{3h} symmetry. This system is analogous to Nb₃C₂, which has been studied in spectroscopic detail by Yang et al. using PFI-ZEKE.⁴ Structurally, the isovalent species are identical to one another with the cation having a highly symmetric trigonal bipyramid structure in which both carbon atoms are triply bound to either side of the equilateral metal face. Addition of another electron into a degenerate orbital leads to Jahn-Teller distortion into lower symmetry and both carbon atoms remain triply bound to the three metal atoms. The Mulliken analysis shows that the metal-

carbon bonding changes very little upon ionization. However, the metal-metal bonding changes significantly, where the Ta-Ta' and Ta'-Ta'' bonds gain significant bonding character in the cation. The atomic charges for two of the metal atoms gain by ~0.33 each and the third gains 0.24. The two carbon atoms each gain 0.06 of the charge.

The doublet state (C_s) shown in Table 2 is the same structure as that reported previously for Ta₃C₃.¹⁰ In the cation, the lowest energy state has singlet multiplicity and C_s symmetry. Both structures consist of one carbon atom triply bridged across the three metal atoms, and the other two carbon atoms are bound across a metal-metal bond and face away from top carbon atom. The population analysis indicates that all three C atoms decrease the bonding population with the metal atoms upon ionization, and the metal-metal bonding is similarly weakened. The atomic charges in the cation show that two of the metal atoms gain 0.33 each and the third gains 0.30. The two C' atoms lose 0.04 of the charge each, but the C atom gains 0.03, increasing from -0.51 to -0.55 upon ionization.

For Ta₄, we previously calculated a singlet state with C_{2v} symmetry to be lowest in energy.¹⁰ More recently, as part of an investigation into mixed-metal clusters, we have recalculated a higher symmetry T_d singlet state that is 128 kJ/mol lower in energy.¹⁸ For the cation, we find the lowest energy structure to be a doublet state. Although the symmetry is C_{2v}, the structure is only slightly distorted from the tetrahedral structure with a dihedral angle of 69°. Because of the relative high symmetry of the neutral, the Mulliken population shows that all Ta atoms have zero charge. Upon ionization, the Ta' pair gains 0.23 and the Ta pair gains 0.27 of the net charge. Furthermore, four of the bonds slightly increase in bonding character and two slightly decrease.

The singlet state calculated previously (C_s) remains the lowest energy structure for Ta₄C.¹⁰ The lowest energy cation is a doublet state (C_s) state with a structure similar to the neutral. The carbon atom is doubly bridged across the Ta'-Ta' bond. The metal framework has opened slightly with a dihedral angle of 77° and 76° for the neutral and cation, respectively. The bonding analysis reveals that the metal-carbon bonding and metal-metal bonding is similar in both the neutral and cation. All four metal atoms experience approximately the same increase in atomic net charge, ~0.25 each, upon ionization although they have quite different initial charges. The C atom also increases the net charge very slightly.

The lowest energy structure for neutral Ta₄C₂ is the same as that calculated previously;¹⁰ a singlet state with no symmetry (C₁). One tantalum atom (Ta) retains bonds to the other three metal atoms. The C atom is triply bridged, and the C' atom is doubly bridged. The cation is a doublet state, also with no symmetry (C₁) but both carbon atoms are now triply bridged as reflected in the Mulliken population, although the Ta'-C bond is much weaker than the other two bonds. Another change is that the Ta atom has bonding density to all other metal atoms in the neutral but the Ta-Ta'' and Ta-Ta''' interactions become antibonding in the cation. Upon ionization, the four metal atoms gain 0.3, 0.28, 0.24, and 0.23 charges. The C atom gains 0.02 but the C' atom loses charge, becoming more electronegative by 0.07 in the cation.

For neutral Ta₄C₃, we calculate a singlet state (C_{3v}) that is 184 kJ/mol lower than the singlet state reported previously (C_{2v}).¹⁰ The cation is a doublet state with reduced C_s^{*} symmetry. In both structures, all carbon atoms are triply bridged; however, the three Ta'-Ta' bonds in the neutral have become substantially weaker in the cation, as reflected in the Mulliken population.

TABLE 5: Summary of Mulliken Bonding Population and Mulliken Charges for Ta₄C_n Neutral (Normal) and Cationic (Bold) Clusters^a

Ta ₄	Ta/Ta'	Ta	Ta/Ta'	Ta	charge (neutral)	charge (cation)
Ta/Ta'		0.245	0.223	0.245	0.000	0.227
Ta	0.231		0.245	0.229	0.000	0.273
Ta/Ta'	0.231	0.231		0.245	0.000	0.227
Ta	0.231	0.231	0.231		0.000	0.273

Ta ₄ C	Ta	Ta'	Ta'	Ta''	C	charge (neutral)	charge (cation)
Ta		0.189	0.189	0.246	0.032	0.076	0.340
Ta'	0.163		0.003	0.238	0.358	0.168	0.412
Ta'	0.163	-0.007		0.238	0.358	0.168	0.412
Ta''	0.254	0.273	0.273		-0.136	0.027	0.262
C	0.066	0.366	0.366	-0.153		-0.438	-0.426

Ta ₄ C ₂	Ta	Ta'	Ta''	Ta'''	C	C'	charge (neutral)	charge (cation)
Ta		0.294	-0.003	-0.080	-0.102	0.258	0.181	0.485
Ta'	0.291		0.100	0.091	0.101	-0.179	0.169	0.449
Ta''	0.144	0.101		-0.082	0.294	0.218	0.270	0.498
Ta'''	0.159	0.000	-0.096		0.317	0.280	0.297	0.536
C	-0.174	0.343	0.145	0.292		-0.060	-0.470	-0.453
C'	0.069	-0.109	0.332	0.375	-0.053		-0.447	-0.514

Ta ₄ C ₃	Ta'	Ta'/Ta''	Ta'/Ta''	Ta	C/C'	C/C'	C	charge (neutral)	charge (cation)
Ta'		0.040	0.041	-0.127	-0.146	0.233	0.233	0.368	0.608
Ta'/Ta''	0.114		0.042	-0.125	0.233	-0.146	0.232	0.369	0.608
Ta'/Ta''	0.114	0.114		-0.125	0.232	0.233	-0.147	0.369	0.608
Ta	-0.127	-0.127	-0.127		0.282	0.281	0.281	0.428	0.680
C/C'	-0.153	0.251	0.251	0.324		-0.074	-0.074	-0.511	-0.501
C/C'	0.251	-0.153	0.251	0.324	-0.077		-0.074	-0.511	-0.502
C	0.251	0.251	-0.153	0.324	-0.077	-0.077		-0.511	-0.502

Ta ₄ C ₄	Ta	Ta'	Ta''	Ta/Ta'''	C	C''	C'	C/C'''	charge (neutral)	charge (cation)
Ta		-0.129	-0.130	-0.097	-0.138	0.245	0.249	0.287	0.508	0.722
Ta'	-0.188		-0.097	-0.130	0.245	-0.138	0.287	0.249	0.537	0.722
Ta''	-0.171	-0.053		-0.129	0.249	0.287	-0.138	0.245	0.613	0.722
Ta/Ta'''	-0.122	-0.188	-0.171		0.287	0.249	0.245	-0.138	0.507	0.722
C	-0.111	0.236	0.258	0.277		-0.075	-0.073	-0.061	-0.535	-0.472
C''	0.235	-0.113	0.322	0.236	-0.085		-0.061	-0.073	-0.537	-0.472
C'	0.257	0.310	-0.145	0.257	-0.089	-0.068		-0.075	-0.558	-0.472
C/C'''	0.277	0.236	0.258	-0.111	-0.060	-0.085	-0.089		-0.535	-0.472

^a 1st/2nd atom label corresponds to neutral and cation, respectively.

The metal–carbon bonding is only slightly reduced relative to the neutral. The overall charge increase upon ionization is even for all metal atoms, ~ 0.24 each, and the carbon atoms gain an insignificant charge of 0.01 each.

We now calculate the lowest energy state of neutral Ta₄C₄ to be a triplet state with C_s* symmetry. This state is 51 kJ/mol lower in energy than the singlet C_{2v} state reported previously by us.¹⁰ The cation is a doublet state with D₂ symmetry, and the overall bonding is similar to the neutral. As stated previously, these structure can be thought of as face-centered cubes and are examples of the smallest possible three-dimensional structure, a 2 × 2 × 2 nanocrystal.¹⁰ The bonding population for the neutral cluster indicates that all metal–metal interactions are antibonding and each carbon atom is triply bridged to each of the four faces. The overall bonding in the cation is similar to the neutral. Upon ionization, the metal atoms gain quite different amounts of charge, 0.21, 0.19, 0.11, and 0.22 for Ta, Ta', Ta'', and Ta''', respectively. Three of the carbon atoms gain 0.06 and one gains 0.09 of charge, a significant difference to the other Ta₄C_n clusters.

C. Ionization Potentials and the Isolobal Valence Bond Model. The adiabatic ionization energies are calculated as the difference in energy between the neutral and cation of each

cluster and are listed in Table 1. (Note that although ionization energies both excluding and including zero point energies are listed in the Table, only the latter numbers will be considered for discussion.) From Table 1, it is seen that the absolute calculated IPs (including ZPE) for Ta₃ and Ta₄ are 6.267 and 6.218 eV, respectively, which are (i) both higher than the experimental values and (ii) similar to each other, that is, the tetramer value is not higher than the trimer as observed experimentally. Regarding the first point, the absolute values of the calculated IPs for all these species are approximately 0.5 eV too high employing the method described here. We have also found this to be the case for our calculations on Nb₃CO and Nb₃(CO)₂, which were both ~ 1 eV higher than the experimental values.²⁹ By substituting other methods that utilize slightly different exchange and correlation functionals (i.e., MPW1PW91 and B3LYP) we have been able to achieve closer absolute IPs for these species. However, we follow the lead of Yang et al. who use the B3P86 method because it gives the best overall match to the electronic, geometric, and vibrational structure of the few benchmark metal–carbide clusters for which this information is known, namely, Nb₃C₂ and Y₃C₂.^{4,25} Moreover, it is the effect on IP of adding carbon atoms to the cluster that is important in this study and so we consider the

change in IP, Δ IP. Similar reasoning can be applied to the second point, that is, that the IP of Ta_4 is calculated to be similar to, and not higher than, the IP of Ta_3 . We have not undertaken a systematic survey of computational methods for calculating absolute IPs; rather, we are interested in the effect of adding carbon atoms onto the Ta_3 and Ta_4 moieties, respectively.

In addition to the experimental IPs, Figure 4 also shows the calculated Δ IP for each Ta_3C_n (Δ) and Ta_4C_n (\square) cluster. A linear offset has been applied to the calculated IPs of Ta_3 (-0.67 eV) and Ta_4 (-0.39 eV) to overlap it with the experimental values. As can be seen clearly, the experimental oscillatory trend is followed very closely. As discussed above, none of the calculated structures have a molecular C_2 group, asserting our postulation that the oscillatory IP pattern is not due to a severe change in bonding/geometry as additional carbon atoms are attached. Although we have not calculated the IPs that would result for clusters containing molecular C_2 groups, we do calculate that the energies of such structures are much higher and are therefore unlikely to be present under molecular beam conditions.

For Ta_3C , it is the transition originating from the doublet state, $S = 1/2 \rightarrow S = 0$, that is included in Figure 4 despite the fact that we calculate it to be ~ 5 kJ/mol higher in energy than the quartet state. The $S = 3/2 \rightarrow S = 1$ transition occurs >0.6 eV higher in energy (see Table 1) and clearly does not fit the experimental results. Similarly, the $S = 1/2 \rightarrow S = 1$ transition is also too high in energy (Table 1). Because of the nature of the PIE experiment, which is sensitive only to the lowest energy ionization process, it is appropriate to consider the doublet state as long as it has some thermal population present in the molecular beam. Although higher energy ionization processes may occur, these would be masked by the rising efficiency of the lowest energy ionization process and therefore not be evident. Hence, we contend that the experimentally determined IP should be compared to system I, the $S = 1/2 \rightarrow S = 0$ transition.

Because the calculated IPs are in agreement with the experimental values, it should be possible to determine the underlying explanation for the oscillatory IP trend that is observed/predicted for clusters with even/odd numbers of carbon atoms. Because the IP is a reflection of the amount of energy required to extract an electron from the neutral, a simple approach is to look to the energy of the HOMO (insofar that the DFT calculation includes Hartree–Fock molecular orbitals) for a correlation with the IP. Although we do not present their energies, we find no correlation found between the HOMO energy and the IP. It is apparent that significant reordering of the electronic arrangement occurs upon ionization that cannot be explained with a single electron treatment, that is, Koopmans' rule does not hold.

An alternative approach is to consider the valence bond model developed by Wade, Mingos, and others for condensed-phase metal-cluster compounds.³⁰ The model considers edge-localized, two-electron, two-center bonds, and the frontier orbitals of each atom available for bonding are represented as isolobal fragments. These fragments can be used in metal–carbide clusters because the nodal characteristics of the frontier orbitals are similar for main group elements and transition metals. We consider each metal atom to contribute 5 valence electrons and be either 4-coordinate (sd^3) or 3-coordinate (sd^2). In the former, there are $1 \times \sigma$ -type (s: d_z^2), $2 \times \pi$ -type (d_{xz} , d_{xy}) and $1 \times \delta$ -type ($d_{x^2-y^2}$: d_{xy}) hybrid orbitals. For a coordination of 3, there are $1 \times \sigma$ -type (s: d_z^2) and $2 \times \pi$ -type (d_{xz} , d_{xy}) hybrid orbitals. Each carbon is sp^3 hybridized and contributes 2 or 0 valence

electrons depending whether it is 3-coordinate ($1 \times \sigma$ -type and $2 \times \pi$ -type orbitals, and 1 lone pair) or 2-coordinate ($1 \times \sigma$ -type and $1 \times \pi$ -type orbital, and 2 lone pairs respectively). The metal's δ -type orbitals can be used only for metal–metal bonding because there is no corresponding δ orbital contained on carbon. The localized description is valid only when the number of edges radiating from each vertex is equal to, or less than, the number of valence orbitals available for bonding.³⁰ Because all of the calculated geometries in Section IIIB consist of carbon atoms with a maximum coordination of 3 and metal atoms with a maximum coordination of 4, this choice of valence bonding method is appropriate.

We assume that the geometries are the same as our calculated structures and that they have the maximum symmetry. The valence electrons are used to fill in the maximum number of metal–carbon bonds permitted by the geometry and then the metal–metal bonds. If any electrons remain, two electrons are assigned as a localized nonbonding pair to any metal atom that is only 3-coordinate. If all metal atoms are already 4-coordinate, the remaining electrons are considered antibonding. Because a 3-coordinate carbon supplies 3 valence orbitals but can donate only 2 electrons to cluster bonding, we consider metal–carbon interactions to be a mixture of ionic and covalent bonding.

If we follow this procedure for Ta_3C_2 and Ta_4C_2 , we find that all metal atoms can be 4-coordinate (all bonding) and all carbon atoms 3-coordinate. However, in both cases we have remaining electrons that are situated in antibonding orbitals (1 and 2 electrons, respectively). This is the reason that the IPs of these clusters are low, because the removal of an electron in these two clusters stabilizes the cation. In the case of Ta_3C_2 , ionization creates a closed-shell structure. This bonding pattern can be seen in the Mulliken bonding population for Ta_3C_2 , where in the neutral there exists a repulsive interaction between two metal atoms; however, upon ionization this interaction now becomes attractive.

In the case of Ta_3C_3 , we observe that the structure allows only 1 carbon to be 3-coordinate, while the remaining 2 are 2-coordinate. Upon filling of the valence electrons, we conclude that there are three electrons remaining for metal–metal bonds and because of the symmetry of the cluster a bond is present between the degenerate metal atoms. This is observed in the Mulliken bonding population, where between the three metal atoms there is one attractive interaction and two repulsive. We conclude that this cluster has a high IP because ionization removes a bonding electron destabilizing the cation relative to the neutral. This pattern is observed in the Mulliken analysis where there is a decrease in attraction between both metal–metal and metal–carbon interactions.

Using the calculated geometries of Ta_3C , Ta_4C , and Ta_4C_3 , once all the bonding electrons are filled there remains enough 3-coordinate metal atoms to accommodate nonbonding electrons. For Ta_3C and Ta_4C , this is oversimplified because there are additional higher order metal–metal bonds (i.e., π and δ bonds) not able to be represented by hybrid orbitals. This is supported by the Mulliken bonding population for both Ta_3C and Ta_4C , where some metal–metal interactions are stronger than others. This may explain why each carbon atom is only 2-coordinate. For Ta_3C and Ta_4C , we still believe there are nonbonding electrons. For Ta_4C_3 , where all C atoms are 3-coordinate and three Ta atoms are 4-coordinate, the remaining two electrons are nonbonding on the 3-coordinate metal atom. We contend that these nonbonding electrons are localized, of similar energy to nonbonding electrons on the bare metal cluster. Upon ionization, the removal of such an electron results in an

unchanged IP relative to the bare metal cluster. This reasoning is similar to that used to explain why the IPs of Nb_nO_m clusters are unaffected by the addition of oxygen atoms because “the IP is little affected by the strongly bonding interactions as the HOMO is an essentially nonbonding metal-centred orbital”.²⁴

For Ta_4C_4 , we assume T_d symmetry. All metal and carbon atoms are now 3-coordinate. Because of the T_d symmetry and all the metal atoms having free δ -type orbitals, the remaining four valence electrons can become delocalized over the entire cluster. This is consistent with early HF calculations and more recent DFT calculations on Nb_4C_4 .^{31,32} This delocalization enables an electron to be removed easily because the resulting charge is distributed easily, resulting in a very low IP. The Mulliken bonding analysis shows all metal interactions to be repulsive in the neutral, whereas upon ionization there is an overall significant decrease in the metal–metal repulsion, thus stabilizing the cation and resulting in a low IP. From this bonding analysis, the delocalized electrons can therefore be considered antibonding and, similar to our argument above for Ta_3C_2 and Ta_4C_2 , result in a stabilized cation and therefore a lower IP.

It is interesting that for Ta_3C_2 , Ta_4C_2 , and Ta_4C_4 , which we consider to have “low” IPs, all metal atoms within the cluster have equal coordination (4, 4, and 3, respectively). For the cations of the two clusters we consider lowest in their respective series (Ta_3C_2 and Ta_4C_4), we can see that all metal atom bonding is equivalent, leading to maximum symmetry (assuming the ideal case of D_{3h} and T_d , respectively) and consequently to have zero dipole. This can also be considered from the perspective of the thermodynamic cycle: $IP(Ta_n) - IP(Ta_nC_m) = D_0(Ta_n^+ - C_m) - D_0(Ta_n - C_m)$. If the IP of a particular metal carbide cluster is less than the IP for the bare metal cluster, then the metal–carbon bonding is stronger in the cation than the neutral. For Ta_4C_4 , the face-centered cubic structure of the cation is similar to other solids such as NaCl that are electrostatically bound. Hence, increased charge separation (through ionization) in a symmetric environment enhances the electrostatic interaction between the electropositive metal and electronegative carbon atoms leading to stronger metal–carbon bonding.

IV. Conclusions

We have recorded the IPs for a series of Ta_3C_n ($n = 1-3$) and Ta_4C_n ($n = 1-4$) clusters using photoionization efficiency experiments. We observe an oscillation in the IP that corresponds to an even and odd number of carbon atoms in the cluster. We have also calculated the energetically lowest-lying neutral, and cationic clusters of the same stoichiometry, using DFT. Changes in experimental IP, as additional carbon atoms are added, correlate well with those calculated by DFT, suggesting that differences in electronic structure, and therefore geometric structures, that arise upon ionization are rationalized correctly by theory. Therefore, we show that experimental cluster IPs can be used to validate theoretically calculated geometries of metal–carbide clusters. In this case, further evidence is provided that the Ta_4C_4 cluster has a structure that is, or close to, a $2 \times 2 \times 2$ face-centered cube, the smallest possible type of nanocrystal. Application of a simple valence bond theory assuming isolobal frontier orbitals can also be applied to understand the relative shift in transition energies (the IP) between the neutral and cation for the range of tantalum–carbide clusters examined here.

Acknowledgment. Financial support from the The University of Adelaide’s Faculty of Sciences is gratefully acknowl-

edged. Support from the Australian Research Council for the purchase and maintenance of our lasers is also acknowledged. Computing resources provided by the Australian Partnership for Advanced Computing (APAC) and South Australian Centre for Parallel Computing (SACPC) is also gratefully acknowledged. Thanks also to Mr Alexander Gentleman for assistance with the tables summarizing the computational results.

Supporting Information Available: The supporting tables provide complete geometric parameters for structures shown in Tables 2 and 3 in the main body of the text. This material is available free of charge via the Internet at <http://pubs.acs.org>.

References and Notes

- (1) *Spectroscopy and Dynamics*; Duncan, M. A., Ed.; Jai Press Inc.: Greenwich, CT, 1993; Vol. 1.
- (2) *Cluster Reactions*; Duncan, M. A., Ed.; Jai Press Inc.: Greenwich, CT, 1994; Vol. 2.
- (3) *Spectroscopy and Structure*; Duncan, M. A., Ed.; Jai Press Inc.: Greenwich, CT, 1995; Vol. 3.
- (4) Simard, B.; Mitchell, S. A.; Rayner, D. M.; Yang, D.-S. In *Metal–Ligand Interactions in Chemistry, Physics and Biology*; Russo, N., Salahub, D. R., Eds.; Kluwer Academic Publishers: Dordrecht, The Netherlands, 2000; pp 239–294.
- (5) Guo, B. C.; Kerns, K. P.; Castleman, A. W., Jr. *Science* **1992**, *255*, 1411–1413.
- (6) Guo, B. C.; Wei, S.; Purnell, P.; Buzza, S.; Castleman, A. W., Jr. *Science* **1992**, *256*, 515–516.
- (7) Wei, S.; Guo, B. C.; Deng, H. T.; Kerns, K.; Purnell, J.; Buzza, S. A.; Castleman, A. W., Jr. *J. Am. Chem. Soc.* **1994**, *116*, 4475–4476.
- (8) Pilgrim, J. S.; Brock, L. R.; Duncan, M. A. *J. Phys. Chem.* **1995**, *99*, 544–550.
- (9) Wei, S.; Guo, B. C.; Purnell, J.; Buzza, S.; Castleman, A. W., Jr. *Science* **1992**, *256*, 818–820.
- (10) Heaven, M. W.; Stewart, G. M.; Buntine, M. A.; Metha, G. F. *J. Phys. Chem. A* **2000**, *104*, 3308–3316.
- (11) van Heijnsbergen, D.; von Helden, G.; Duncan, M. A.; van Roij, A. J. A.; Meijer, G. *Phys. Rev. Lett.* **1999**, *83*, 4983–4986.
- (12) von Helden, G.; Tielens, A. G. G. M.; van Heijnsbergen, D.; Duncan, M. A.; Hony, S.; Waters, L. B. F. M.; Meijer, G. *Science* **2000**, *288*, 313–316.
- (13) von Helden, G.; van Heijnsbergen, D.; Duncan, M. A.; Meijer, G. *Chem. Phys. Lett.* **2001**, *333*, 350–357.
- (14) van Heijnsbergen, D.; Fielicke, A.; Meijer, G.; von Helden, G. *Phys. Rev. Lett.* **2002**, *89*.
- (15) Frisch, M. J.; Trucks, G. W.; Schlegel, H. B.; Scuseria, G. E.; Robb, M. A.; Cheeseman, J. R.; Zakrzewski, V. G.; Montgomery, J. A., Jr.; Stratmann, R. E.; Burant, J. C.; Dapprich, S.; Millam, J. M.; Daniels, A. D.; Kudin, K. N.; Strain, M. C.; Farkas, O.; Tomasi, J.; Barone, V.; Cossi, M.; Cammi, R.; Mennucci, B.; Pomelli, C.; Adamo, C.; Clifford, S.; Ochterski, J.; Petersson, G. A.; Ayala, P. Y.; Cui, Q.; Morokuma, K.; Malick, D. K.; Rabuck, A. D.; Raghavachari, K.; Foresman, J. B.; Cioslowski, J.; Ortiz, J. V.; Stefanov, B. B.; Liu, G.; Liashenko, A.; Piskorz, P.; Komaromi, I.; Gomperts, R.; Martin, R. L.; Fox, D. J.; Keith, T.; Al-Laham, M. A.; Peng, C. Y.; Nanayakkara, A.; Gonzalez, C.; Challacombe, M.; Gill, P. M. W.; Johnson, B. G.; Chen, W.; Wong, M. W.; Andres, J. L.; Head-Gordon, M.; Replogle, E. S.; Pople, J. A. *Gaussian 98*, revision x.x.; Gaussian, Inc.: Pittsburgh, PA, 1998.
- (16) *Gaussian Basis Sets for Molecular Calculations*; Huzinaga, S., Ed.; Elsevier: Amsterdam, 1984; Vol. 16.
- (17) Hay, P. J.; Wadt, W. R. *J. Chem. Phys.* **1985**, *82*, 270–283.
- (18) Addicoat, M. A.; Buntine, M. A.; Metha, G. F. *Aust. J. Chem.* **2004**, *57*, 1197–1203.
- (19) Németh, G. I.; Ungar, H.; Yeretzyan, C.; Selzle, H. L.; Schlag, E. W. *Chem. Phys. Lett.* **1994**, *228*, 1–8.
- (20) Collings, B. A.; Rayner, D. M.; Hackett, P. A. *Int. J. Mass. Spec. Ion Proc.* **1993**, *125*, 207–214.
- (21) Zakin, M.; Cox, D.; Whetten, R.; Trevor, D.; Kaldor, A. *Chem. Phys. Lett.* **1987**, *135*, 223–228.
- (22) Yang, D. S.; James, A. M.; Rayner, D. M.; Hackett, P. A. *Chem. Phys. Lett.* **1994**, *231*, 177–182.
- (23) Knickelbein, M.; Yang, S. *J. Chem. Phys.* **1990**, *93*, 5760–5767.
- (24) Athanassenas, K.; Kreisle, D.; Collings, B. A.; Rayner, D. M.; Hackett, P. A. *Chem. Phys. Lett.* **1993**, *213*, 105–110.
- (25) Yang, D.-S.; Zgierski, M. Z.; Bérces, A.; Hackett, P. A.; Roy, P.-N.; Martinez, A.; Carrington, T., Jr.; Salahub, D. R.; Fournier, R.; Pang, T.; Chen, C. *J. Chem. Phys.* **1996**, *105*, 10663–10671.
- (26) Knickelbein, M. B.; Menezes, W. J. C. *Chem. Phys. Lett.* **1991**, *184*, 433–438.

- (27) Knickelbein, M. B. *Annu. Rev. Phys. Chem.* **1999**, *50*, 79–115.
- (28) Fang, L.; Shen, X.; Chen, X.; Lombardi, J. R. *Chem. Phys. Lett.* **2000**, *332*, 299–302.
- (29) Pedersen, D. B.; Rayner, D. M.; Simard, B.; Addicoat, M. A.; Buntine, M. A.; Metha, G. F.; Fielicke, A. *J. Phys. Chem. A* **2004**, *108*, 964–970.
- (30) *Introduction to Cluster Chemistry*; Mingos, D. M. P., Wales, D. J., Ed.; Prentice Hall Inc.: New Jersey, 1990.
- (31) Yeh, C. S.; Byun, Y. G.; Afzaal, S.; Kan, S. Z.; Lee, S.; Freiser, B. S.; Hay, P. J. *J. Am. Chem. Soc.* **1995**, *117*, 4042–4048.
- (32) Harris, H.; Dance, I. *J. Phys. Chem. A* **2001**, *105*, 3340–3358.